Optical and Thermo-optical Properties of Polyimide-Single-Walled Carbon Nanotube Films: Experimental Results and Empirical Equations

Joseph G. Smith Jr.,[†,*] *John W. Connell,*[†] *Kent A. Watson,*[‡] *and Paul M. Danehy*[§]

NASA Langley Research Center, Advanced Materials and Processing Branch, Mail Stop 226 and Advanced Sensing and Optical Measurement Branch, Mail Stop 493, Hampton, VA 23681-2199 and National Institute of Aerospace Research Associate, 144 Research Drive, Hampton, VA 23666

The incorporation of single-walled carbon nanotubes (SWNTs) into the bulk of space environmentally durable polymers at loading levels ≥0.05 wt % has afforded thin films with surface and volume resistivities sufficient for electrostatic charge mitigation. However, the optical transparency at 500 nm decreased and the thermo-optical properties (solar absorptivity and thermal emissivity) increased with increaed SWNT loading. These properties were also dependent on film thickness. The absorbance characteristics of the films as a function of SWNT loading and film thickness were measured and determined to follow the classical Beer-Lambert law. Based on these results, an empirical relationship was derived and molar absorptivities determined for both the SWNTs and polymer matrix to provide a predictive approximation of these properties. The molar absorptivity deteermined for SWNTs dispersed in the polymer was comparable to reported solution determined values for HiPco SWNTs.

Corresponding author. E-mail: Joseph.G.Smith@NASA.gov

† NASA Langley Research Center, Advanced Materials and Processing Branch

§ NASA Langley Research Center, Advanced Sensing and Optical Measurement Branch

‡National Institute of Aerospace

Introduction

Space durable polymeric films are one of several enabling technologies for Gossamer spacecraft.[1] These vehicles are large, deployable and ultra-lightweight and would be partially constructed of polymer films. To be durable to the space environment, the film needs to exhibit resistance to electrons, protons, and UV and vacuum UV radiation. For some applications, the film must also possess low solar absorptivity (i.e. low-color), optical transparency across the visible spectrum (particularly at 500 nm), and high thermal emissivity ( ). Optical transparency at 500 nm is of interest since this is the wavelength at which the solar maximum occurs. The solar absorptivity ( ) pertains to the fraction of incoming solar energy that is absorbed by the film and is typically low for a low color film. The is a measure of the film's ability to radiate energy from the film surface. Films that exhibit low and high values are desirable since little radiation would be absorbed while most of the radiation impinging upon it would be radiated away from the surface. It is known that these properties are dependent upon film thickness and inclusion of an absorbing species.

In addition to the aforementioned properties, intrinsic electrical conductivity (measured as resisitivity) is needed to mitigate electrostatic charge (ESC) accumulation. ESC build-up occurs upon exposure of insulating materials such as polymers to a charged orbital environment. When discharge occurs, damage to surrounding materials and electronics on the spacecraft can result. The level of surface resistivity required to mitigate ESC accumulation is in the range of 10^6-10^{10} /square.[2]

Due to their exceptional physical and mechanical properties as well as radiation resistance, aromatic polyimides are excellent materials for these applications. Respectable space environmental durability and low color and have been attained by proper choice of the constituent monomers.[3,4] Sufficient intrinsic conductivity (measured as resisitivity) for ESC mitigation has been achieved by the incorporation of SWNTs into the bulk[5-10] of space durable polymers (e.g. TOR-NC , LaRC™ CP-2, and modified LaRC™ CP-2) as well as a surface coating.[11] Bulk inclusion of SWNTs afforded films that exhibited both surface and volume resistivity. Surface coating afforded only one conductive side (measured as resisitivity) with the bulk and opposing side being insulative.

It was found that surface coating of SWNTs had a negligible effect upon the optical transparency, , and compared to the pristine material.[11] However, bulk inclusion of SWNTs at the loading levels necessary to reach the electrical percolation threshold caused significant darkening resulting in decreased % transmission (%T) at 500 nm and increased and for films of approximately the same thickness.[5,7,10] The absorbance at 500 nm and of the SWNTs included in the bulk of the polymer was observed to follow the classic Beer's law equation when plotted vs. wt % SWNT loading. Similar results were obtained for SWNTs (produced by the HiPco process) "dissolved" or "suspended" in 1,2-dichlorobenzene[12] and for functionalized SWNTs (produced by arc discharge) dissolved in solution.[13] In all cases, light scattering due to the SWNT bundles affected the results. For film samples, the results were also affected by reflectivity losses at the polymer-air interface.

Due to the adherence of the nanocomposites to Beer's law, it was of interest to further examine this effect and attempt to develop a predictive empirical eq for these properties (absorbance and). This is important given that ultra-thin films (<3 m) would be needed for proposed Gossamer strucutres. In this work, nanocomposite films of an alkoxysilane terminated LaRC™ CP-2 polymer and purified high-pressure carbon monoxide (HiPco) SWNTs were prepared to evaluate the effects of SWNT incorporation upon the optical transparency at 500 nm, , and . This was performed at different SWNT

loadings and film thickness. The data was subsequently examined using Beer's (absorbance vs. concentration) and Lambert's (absorbance vs. film thickness) laws with the results described herein.

Experimental Section

Materials. The following chemicals were obtained from the indicated sources and used without further purification: aminophenyltrimethoxysilane (APTS, Gelest Inc., ~90% meta, ~10% para), 1,3-bis(3-aminophenoxy)benzene (APB, Mitsui Chemicals America, Inc. mp 107-108.5 °C), and N,N-dimethylacetamide (DMAc, Aldrich). 4,4'-Hexafluoroisopropylidiene diphthalic anhydride (6-FDA, Hoechst Celanese Inc., mp 241-243 °C) was sublimed prior to use. SWNTs prepared by the HiPco process were obtained from Tubes@Rice and purified by heating at 250 °C for ~16 h in a high humidity chamber over moist air followed by Soxhlet extraction with hydrochloric acid (22.2 wt%) for ~24 h. All other chemicals were used as received.

Alkoxysilane Terminated Amide Acid Synthesis. An alkoxysilane terminated amide acid (ASTAA) of LaRC™ CP-2 was prepared by the reaction of 6-FDA with APB and end-capped with APTS at a 2.5% offset. First, APB (6.3870 g, 0.0218 mol) and APTS (0.2390 g, 0.0011 mol) were dissolved in DMAc (7 mL) at room temperature under nitrogen. The flask was subsequently immersed in a room temperature water bath to dissipate the heat of reaction when the dianhydride was added. Then 6-FDA (9.9547 g, 0.0224 mol) was added in one portion as a slurry in DMAc (10 mL) and rinsed in with 18 mL of DMAc to afford a ~33.5% (w/w) solution. The reaction was stirred for ~24 h at room temperature under nitrogen. An aliquot was removed to determine inherent viscosity. The remaining solution was used as is or SWNTs were added as described below.

SWNT-ASTAA Mixture. Nanocomposite solutions were prepared by the addition of a sonicated mixture of SWNTs in DMAc to a pre-weighed ASTAA solution. The SWNT loadings were 0.03, 0.05,

and 0.08 wt % based on the mass of ASTAA. After stirring at room temperature under a nitrogen atmosphere for ~16 h, the solutions were used to cast unoriented thin films. A representative procedure is described.

To a 100 mL round-bottom flask equipped with nitrogen inlet, mechanical stirrer, and drying tube filled with calcium sulfate was charged 11.06 g of an ASTAA solution [~33.5% (w/w)]. In a separate vial, SWNTs (0.0011 g) were placed in 3 mL of DMAc and the mixture sonicated for ~2.5 h in a Degussa-Ney ULTRAsonik 57X cleaner operated at ~50% power and degas levels. The initial temperature of the water bath was ambient and ~40 °C at the conclusion of sonication. The suspended tubes were subsequently added to the stirred mixture of ASTAA at room temperature and rinsed in with 4.5 mL of DMAc to afford an ~20% (w/w) solution. The SWNT loading was 0.03 wt %. The mixture was stirred for ~16 h under a nitrogen atmosphere at room temperature prior to film casting.

Films. DMAc solutions of the ASTAAs (with and without SWNTs as described above) were doctored onto clean, dry plate glass and dried to tack-free forms in a low humidity chamber at ambient temperature. The films on glass were stage cured in a forced air oven at 100, 200, and 300 °C for 1 h each. The films were subsequently removed from the glass plate and characterized.

Characterization. Elemental analysis was performed by Desert Analytics (Tucson, Arizona). Inherent viscosities (η_{inh}) were obtained on a 0.5% (w/v) amide acid solution in DMAc at 25 °C. DSC was conducted on a Shimadzu DSC-50 thermal analyzer. Melting point ranges (tangent of onset to melt and the endothermic peak) were determined by either DSC at a heating rate of 10 °C/min or visually on a Thomas-Hoover capillary melting point apparatus (uncorrected). Film thickness was determined on a Testing Machines, Inc. digital micrometer. UV/VIS/near-IR spectra were obtained on thin films using a Perkin-Elmer Lambda 900 UV/VIS/near-IR spectrometer. The η was measured on thin films using an AZ Technology Model LPSR-300 spectroreflectometer with measurements taken between 250 to 2800

nm. Vapor-deposited aluminum on Kapton® film (1st surface mirror) was used as the reflective reference for air mass 0 per ASTM E903. An AZ Technology Temp 2000A infrared reflectometer was used to measure □. Surface resistivity was determined according to ASTM D-257-99 using a Prostat® PSI-870 Surface Resistance and Resistivity Indicator operating at 9 V and reported as an average of three readings.

RESULTS AND DISCUSSION

Nanocomposite Synthesis. The main objective of this project was to incorporate sufficient electrical conductivity (measured as resitivity) into space durable polymeric films to mitigate ESC without

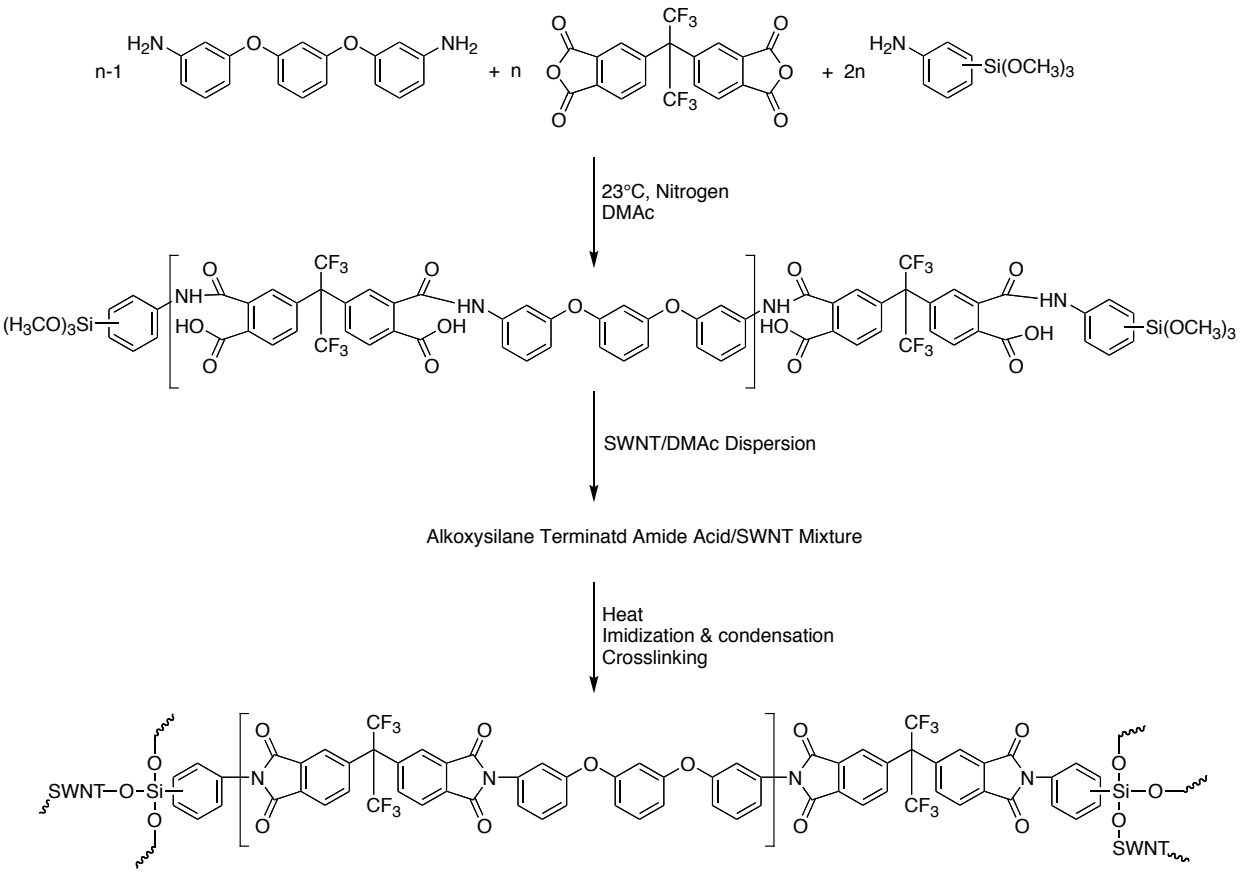

Scheme 1: Polyimide-SWNT nanocomposite synthesis.

detrimental effects to the optical and thermo-optical properties of the pristine material. As previously reported, the method used involved the preparation of an amide acid of a space durable polymer (LaRC™ CP-2) endcapped with latent reactive groups, alkoxysilanes (Scheme 1).[10] The endcapping agent employed was aminophenyltrimethoxysilane. To incorporate sufficient resisitivity for ESC mitigation into the material without affecting other desirable properties, SWNTs were used. The reasons for choosing SWNTs were:

1) their inherent size, which would potentially have a negligible effect upon the thermo-optical and optical properties of the base polymer,
2) their high aspect ratio, which suggests that a relatively low loading level would be needed to reach the electrical percolation threshold, and
3) their high electrical conductivity.

The SWNTs employed in this work were prepared by the HiPco process and purified prior to use. Elemental analysis afforded the following results: 89% C, 0.5% H, and 1.8% Fe. The results imply that not all of the iron was removed. The residual iron is postulated to be due to catalyst entrapped inside the nanotube or encased in an amorphous carbon cage. The remaining mass balance (8.7%) is presumably due to oxygen in the form of carbon-oxygen bonded species such as carboxylic acid and hydroxyl groups[14,15] located at defect sites along the tube or at the tube ends. For these SWNTs, the oxygen content was not determined by elemental analysis.

The SWNTs were added to the ASTAA solution and the mixture stirred under low shear prior to casting unoriented films. The room temperature dried films were stage cured and imidized to 300 °C in flowing air prior to analysis. It was postulated that a chemical reaction would occur between the alkoxylsilane endcap and functionalities on the SWNT due to the purification procedure.[10] Direct observance of any chemical bond formation has been difficult to ascertain based on conventional spectroscopic techniques. The Raman spectra of the SWNTs before and after a model reaction were similar in appearance with slight differences in the radial breathing mode being apparent.[10] Additionally,

analysis by high resolution scanning electron microscopy (HRSEM) revealed a light organic coating on SWNTs that was not present on the purified SWNTs.[10]

The thermal, mechanical, optical, and electrical properties of nanocomposites of approximately the same thickness (38 μm) have been previously reported.[7,10] The η_{inh} of the ASTAA used to prepare the nanocomposite films was 0.88 dL/g (indicative of high molecular weight) with SWNT loadings ranging from 0 to 0.08 wt %. HRSEM suggested that the SWNTs were well dispersed in the matrix with no visible large agglomerates; however, localized regions of low and high SWNT concentration were evident.[10] From that work, a SWNT loading of ≥0.05 wt % was found to afford sufficient surface resistivity necessary for ESC mitigation (Table 1).

Optical and Thermo-optical Properties. It was found that for increasing SWNT loading (P2-P4), the %T at 500 nm decreased while α and βincreased with respect to the pristine material, P1 (Table 1). Additionally, it was determined that the absorbance (A, where $A = 2 - \log_{10}\%T$) adhered to Beer's law when plotted vs. SWNT wt % loading.[10] However, the classic Beer's law eq (A = abc) examines the effect of increasing concentration (c) upon absorbance at constant path length (b). When the concentration is expressed in units of mol/L and the path length in cm, then the absorptivity (a) is the molar absorptivity expressed in units of L/(cm mol). This relationship, originally derived for solutions containing various concentrations of an absorbing species in a cell (typically matching quartz cuvette)s of a constant path length (typically 1 cm), was found to applicable to thin films as well.[16] The plotted data resulted in a non-zero y-intercept and was presumably due to light scattering and reflection in the film.[16] The α, an absorptive property whichencompasses the spectral region ranging from 250-2800 nm, was also found to obey Beer's law even though it was determined using a different instumental setup.[10] Based on the adherence to Beer's law for both absorbance and α, it was of interest to further investigate this effect taking into account reflectivity losses at the film surfaces in order to develop empirical relationships to predict these properties. Losses due to light scattering by SWNT aggregates

and inhomogeneties in the film were not addressed in this study. It has been reported that an accurate determination of scattering contributions to the absorption spectrum by SWNT bundles is very difficult.[13]

Table 1: Optical and Thermo-optical Properties vs. wt % SWNT Loading at Constant Film Thickness[a]

id	SWNT, wt %	film thickness, μm	500 nm %T	A[b]	α	β	s.r.[c] Ω/square
P1	0	38.0	86	0.0655	0.07	0.59	$>10^{12}$
P2	0.03	38.0	67	0.1739	0.21	0.63	10^{11}
P3	0.05	41.0	59	0.2291	0.30	0.65	10^{8}
P4	0.08	38.0	53	0.2757	0.35	0.67	10^{8}

[a] ref 10 [b] $A = 2 - \log_{10}\%T$ [c] s.r. = surface resistivity

The overall goal of this work was to incorporate sufficient intrinsic electrical conductivity (measured as surface resistivity) into a space durable film with minimal effect upon the optical and thermo-properties. The data in Table 1 showed that P3 containing a SWNT loading of 0.05 wt % exhibited sufficient surface resistivity for ESC mitigation. Thus it was of interest to further examine the effect of film thickness at this wt % SWNT loading upon the %T at 500 nm and α. The relationship between thickness and absorbance at constant concentration is known as Lambert's law and, like Beer's law, is based on an absorbing species dissolved in solution. Films of various thickness (P5-P11) were cast from a single nanocomposite mixture prepared from an ASTAA with an η_{inh} of 0.66 dL/g (indicative of moderate to high molecular weight) and a 0.05 wt % SWNT loading with the results reported in Table 2. As expected α and β increased and the %T at 500 nm decreased with increasing

film thickness. Initial plots of absorbance and □ were vs. film thickness were found to obey Lambert's law. However as mentioned above, losses due to reflectivity and light scattering were not taken into account. The surface resistivities were ~10^8 □/square with an order of magnitude increase for P9-P11. These values were comparable to P3. Film P5 had some surface areas

Table 2: Optical and Thermo-optical Properties at Constant wt % SWNT Loading

	SWNT,	film thickness,	500 nm				s.r.,
id	wt %	□m	%T	A	□	□	□/square
P5	0.05	17.5	75	0.1249	0.16	0.47	10^8 - 10^{10}
P6	0.05	22.5	71	0.1487	0.19	0.50	10^8
P7	0.05	35.0	65	0.1871	0.26	0.58	10^8
P8	0.05	37.5	62	0.2076	0.28	0.59	10^8
P9	0.05	55.0	54	0.2676	0.34	0.64	10^7
P10	0.05	67.5	47	0.3279	0.41	0.70	10^7
P11	0.05	82.5	39	0.4089	0.45	0.72	10^7
P12	0	25.0	87	0.0605	0.06	0.46	$>10^{12}$
P13	0	30.0	87	0.0605	0.06	0.51	$>10^{12}$
P14	0	32.5	87	0.0605	0.06	0.51	$>10^{12}$
P15	0	40.0	86	0.0655	0.07	0.55	$>10^{12}$
P16	0	60.0	84	0.0757	0.07	0.62	$>10^{12}$
P17	0	72.5	81	0.0915	0.09	0.65	$>10^{12}$
P18	0	87.5	79	0.1024	0.10	0.68	$>10^{12}$

where the readings were 10^{10} Ω/square implying there were regions of low and high SWNT concentration.

Film thickness effects on %T, α, and β for the neat polymer (P12-P18, Table 2) were also determined. The η_{inh} of the ASTAA was 0.94 dL/g (indicative of high molecular weight) with film thicknesses ranging from 25.0 to 87.5 μm. The %T at 500 nm and α did not vary appreciably for film thicknesses ranging from 25.0 to 40.0 μm (P12-P15) whereas β increased ~20%. Like the SWNT containing films (P5-P11), adherence to Lambert's law was found when absorbance and β were plotted vs. film thickness. As with the other samples, relectivity and light scattering losses were not addressed. Surface resistivities were not determined for P12-P18, since P1 was previously determined to be insulative.

Reflectivity Loss and Modified Eqs. Both Beer's and Lambert's laws pertain to the absorbance at a particular wavelength of a species dissolved in a solution. The experiment is typically performed using matching quartz cuvettes with one cell containg a solvent blank so as to subtract out losses due to solvent and reflectance at the quartz-air interfaces. In this study, the solution is a solid polymer matrix and care has to be taken to account for the Fresnel reflection from the two polymer-air interfaces of the material.[17] Each interface results in a few percent reflection that must be accounted for so this loss of light is not wrongly attributed to absorption or scattering by the medium. The fraction reflected from each surface can be calculated from

$$R = [(n_{LaRC™CP-2} - n_{air})/(n_{LaRC™CP-2} + n_{air})]^2,$$

where R is the reflectivity and $n_{LaRC™CP-2} = 1.61$ and $n_{air} = 1$ are the indices of refraction of LaRC™ CP-2[4] and air, respectively. Thus R = 0.0546 per surface. Considering that the film has two air-polymer surfaces, the *%T* for a sample having zero absorbance was calculated as

$$\%T = 100(1 - 2R) = 89.1\%.$$

Therefore, a modified definition of absorbance was used:

$$A = 2 - \log_{10}(\%T/0.891) \qquad (1)$$

where the 0.891 refers to the 89.1% transmittance. Rearranging eq 1 afforded eq 2.

$$\%T = 89.1(10^{-A}) \qquad (2)$$

The absorbance was recalculated for P1-P18 using eq 1, to take into account losses due to reflection, with the values reported in Table 3.

Normally in analysis of spectrometer data, this modification is not required because a reference scan is usually performed with a sample having the absorbing species absent. For liquid samples, this is relatively easy to accommodate. This reference scan is then used to "zero" the instrument, thereby taking into account these reflective losses from the sample cell-air interfaces. However in the present study, films of varying thickness were used so a single reference scan would not have been appropriate, particularly because the neat polymer itself has absorption and/or scattering losses. Consequently, the modified relationships for absorbance and %T (eqs 1 and 2, respectively) were used.

Complicating matters, both the SWNT and host polymer material exhibit absorption of light at 500 nm. This can be seen in Figure 1, which shows transmission spectra of the neat polymer film (P1) and three different wt % SWNT loadings (P2-P4) in the spectral region ranging from 350-900 nm. The figure shows that %T decreases with increasing SWNT loading. Additionally, there is an obvious drop in transmission towards the ultra-violet end of the spectrum (<400 nm) caused by absorption of the host polymer. The high frequency oscillations in the 0.03 wt % SWNT loading spectrum (P2) are not

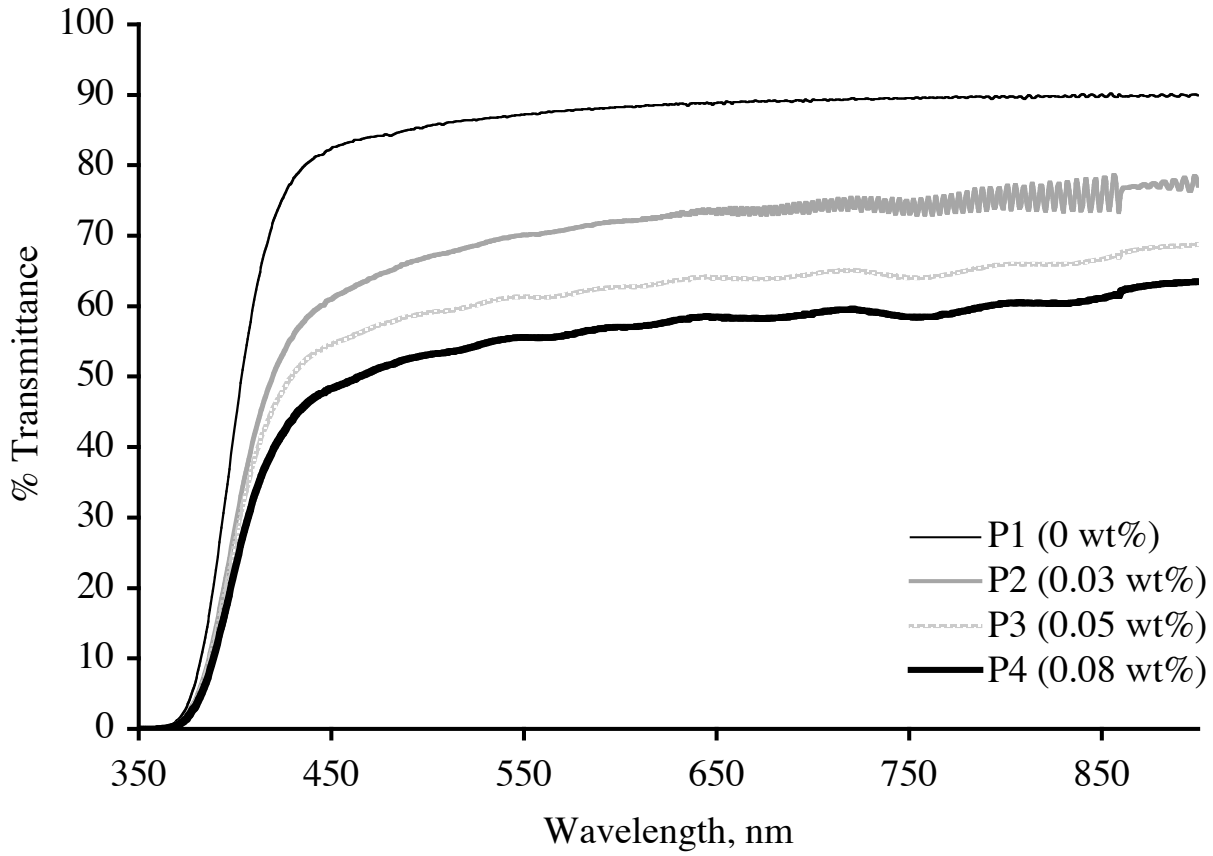

Figure 1. Transmission spectra of P1–P4 with different wt % SWNT loadings but approximately the same thickness (38 μm) except for the 0.05 wt % SWNT loading (P3), which was 41 μm.

repeatable and are believed to be due to noise in the instrument. As seen in Figure 1, it appears that the SWNTs do not exhibit a strong transmission variation with wavelength. In this study though we only report results obtained at 500 nm.

Determination of polymer and SWNT concentration. Since both the SWNT and the host polymer affect the transmission of light through the sample, analysis of the data must include absorptivity of both. Thus, we define a_{SWNT} and a_{host} as the absorptivity of the SWNT and host materials, respectively.

Similarly, we define c_{SWNT} and c_{host} as the concentration of the SWNT and host materials, respectively. Thus, the expression for the absorbance can be written as:

$$A = (a_{host}c_{host} + a_{SWNT}\, c_{SWNT})b. \qquad (3)$$

There are many ways to treat this data from this point. One way is to use wt% SWNT. However, to obtain absorptivity values in units that are traditionally found in the Beer-Lambert law eq we chose to convert the amounts of materials used into units of concentration (mol/L). This would then allow for comparison of absorptivity values determined in the film to those reported in the literature for solutions. First the concentration of the host material (c_{host}) was calculated to be 2.10 mol/L by dividing the density (ρ) of the polymer (1.47 g/mL for LaRC™ CP-2)[3] by the molecular weight of the repeat unit (700.5586 g/mole) and multiplying by 1000. Here it was assumed that the ρ of the modified LaRC™ CP-2 was comparable to that of LaRC™ CP-2, ignoring any contribution from the endcapping group that was present at 5 mol %.

Likewise, the wt % SWNT loading needed to be converted to concentration (mol/L) for c_{SWNT}. This was performed making several assumptions. The first was that SWNTs could be thought of as "essentially" an all carbon polymer. Based on this assumption, the SWNT repeat unit would be 12.0112 g/mol negating minor contributions afforded by oxygen, hydrogen, and residual catalyst(s). The second assumption was that the polymer matrix could be thought of as the "solvent" that the SWNTs were "dissolved" in. Based on these assumptions, an example of converting the SWNT concentration from wt % to mol/L is presented below.

g SWNT = 0.0018 g approximate mol SWNT = g SWNT/(12.0112 g/mol) = 1.5×10^{-4} mol

Repeat unit MW_{ASTAA} = 736.5894 g/mol Repeat unit MW_{imide} = 700.5586 g/mol

Table 3: Absorbance taking into account reflectance

id	c_{SWNT}, mol/L	film thickness, μm	A[a]
P1	0	38.0	0.0152
P2	0.041	38.0	0.1237
P3	0.068	41.0	0.1789
P4	0.100	38.0	0.2255
P5	0.065	17.5	0.0747
P6	0.065	22.5	0.0985
P7	0.065	35.0	0.1368
P8	0.065	37.5	0.1573
P9	0.065	55.0	0.2173
P10	0.065	67.5	0.2776
P11	0.065	82.5	0.3587
P12	0	25.0	0.0102
P13	0	30.0	0.0102
P14	0	32.5	0.0102
P15	0	40.0	0.0152
P16	0	60.0	0.0255
P17	0	72.5	0.0412
P18	0	87.5	0.0521

[a] eq 1: $A = 2 - \log_{10}(\%T/0.891)$

$g_{ASTAA} = 3.3924$ g $\qquad g_{imide} = g_{ASTAA} (MW_{imide} / MW_{ASTAA}) = 3.2265$ g

L_{imide} = amount of Imide used/□ of LaRC™ CP-2

$= (3.2265\ g / 1.47\ g/mL)(\ 1\ L/1000\ mL) = 2.20 \times 10^{-3}\ L$

$c_{SWNT} = (1.5 \times 10^{-4}\ mol\ SWNT) / (2.20 \times 10^{-3}\ L\ \ LaRC™\ CP\text{-}2)$

$= 0.068\ mol/L$ for a 0.05 wt % SWNT loading

The c_{SWNT} was calculated for P2-P11 using the method above with the values reported in Table 3.

Analysis of Transmission Measurements. The data in Tables 1-3 can be summarized into three groups: (i) (P12-P18) variation of film thickness (b) for neat polymer ($c_{SWNT} = 0$), (ii) (P1-P4) variation of c_{SWNT} for a constant film thickness (b, approximately equal to 38 □m), and (iii) (P5-P11) variation of film thickness (b) for a polymer with a constant concentration of SWNT ($c_{SWNT} = 0.065$ mol/L). The first and third groups pertain to Lambert's law while the second group pertains to Beer's law. Since the absorbance, film thickness, and host and SWNT concentrations were known; the only remaining unknowns in eq 3 for each sample were a_{host} and a_{SWNT}. Initial estimates were made for these two values allowing a theoretical estimate of absorbance for each sample. The difference between the empirical prediction of absorbance and the value of absorbance inferred from eq 1 was then computed for each sample. These differences were squared and summed. Utilizing the Solver function in Microsoft Excel, a_{host} and a_{SWNT} were adjusted to minimize the sum of these squares, thereby obtaining a best fit to all of the data simultaneously. Based on this analysis the values for a_{host} and a_{SWNT} were 0.000249 and 0.0562 L/(mol □m), respectively. Thus eq 3 can be written as eq 4:

A□□□0.000522 □m^{-1} + 0.0562 L/(mol □m)c_{SWNT}]b (4).

Eq 4 was then used to calculate the absorbance for three groups with the results graphically compared to the data in Figures 2 and 3.

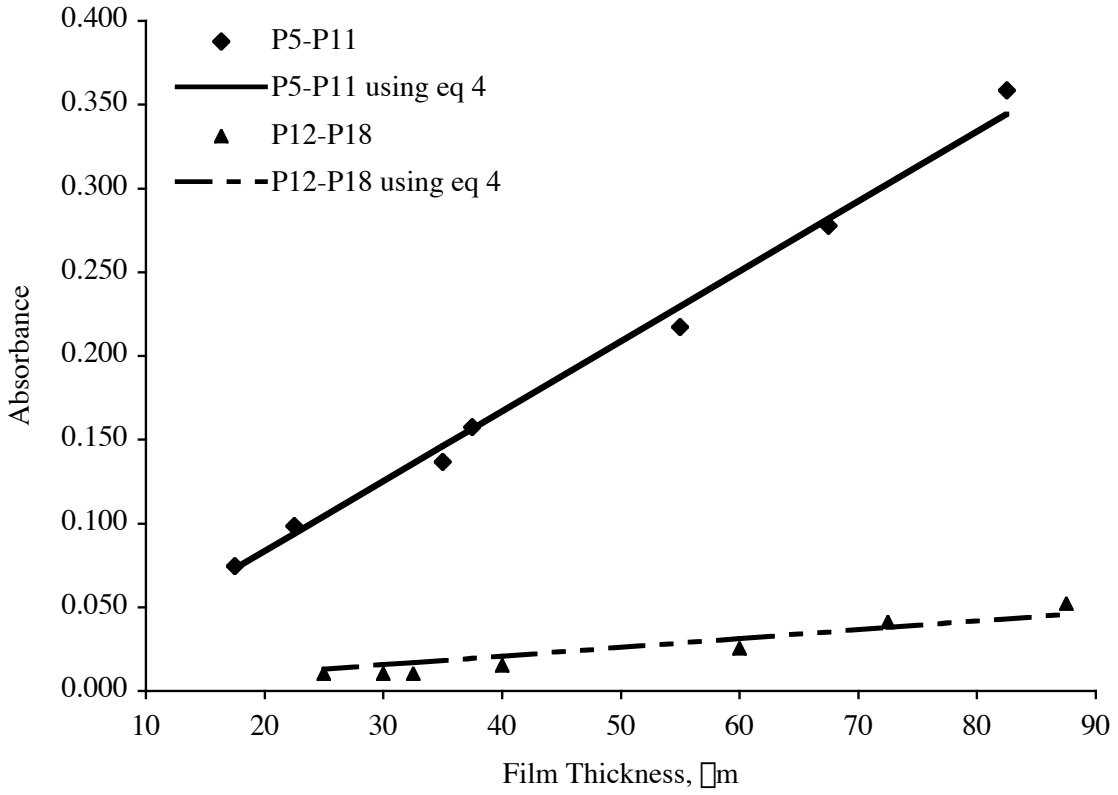

Figure 2. Absorbance vs. film thickness for neat (P12-P18) and SWNT-loaded films (P5-P11).

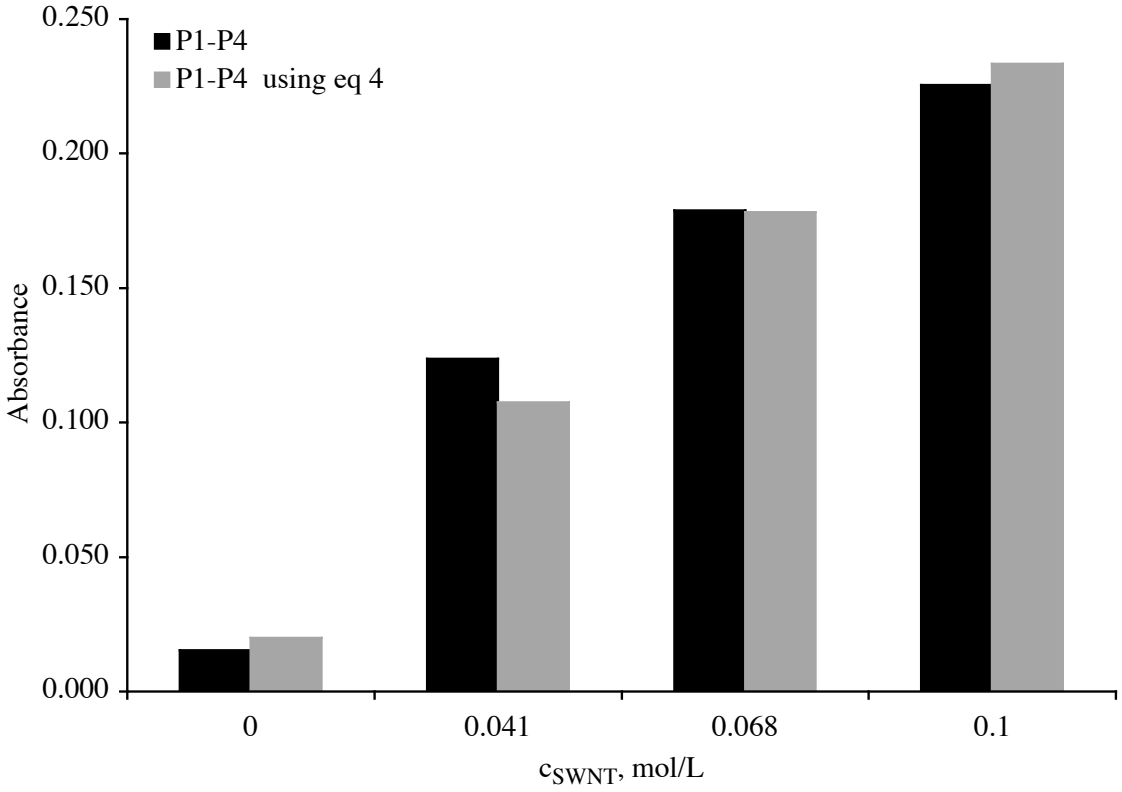

Figure 3. Absorbance vs. c_{SWNT} for approximately constant thickness films (P1-P4).

Figure 2 shows a comparison between eq 4 and the data for absorbance as a function of film thickness, for both neat polymers and nanocomposites, P12-P18 and P5-P11, respectively. As expected, samples containing SWNTs have substantially higher absorbance than neat samples. Furthermore, the absorbance increased with increasing film thickness for samples containing SWNTs. However, it is significant that the neat samples exhibited an increased absorbance with increasing film thickness. This implied that the host material (polymer) was absorbing (or possibly scattering) the incident light. Figure 3 shows a comparison between eq 4 and the data for absorbance versus increasing c_{SWNT}. This graph is shown as a bar graph instead of a line graph because all of the samples were not exactly the same thickness. The expected trend of increasing absorbance with increasing c_{SWNT} was observed.

Generally, the agreement between eq 4 and the data in Figures 2 and 3 was good. The resulting fit values were a_{host} = 0.000249 ± 0.00002 L/(mol μm) and a_{SWNT} = 0.0562 ± 0.002 L/(mol μm). The average deviation between the data and eq 4 (fit standard error) for A was 0.008. Based on this fit standard error, the 95% confidence level of statistical uncertainty in the eq 4 calculation was estimated to be ±0.005 for absorbance, and ±1 for %T using eq 2.

It has been reported that a_{SWNT} at 500 nm of as-produced HiPco SWNTs "dissolved" or "suspended" in 1,2-dichlorobenzene was 0.0286 L/(mg cm).[12] Mathematical conversion of 0.0562 L/(mol □m) obtained in this study to the units of L/(mg cm) afforded a value of 0.0464. This is ~ 60% greater than the reported value, but is of the same order of magnitude and was reasonable given that the SWNT were from a different HiPco batch, purified, and suspended in a solid polymer matrix. Additionally, the former data may have been treated differently (e.g. accounting of scattering). It has been reported that functionalized SWNTs (produced by arc discharge) were insensitive to the medium (solution vs. film)[13] thus allowing for comparisons to be made. An average a_{SWNT} at 500 nm in solution for amide functionalized SWNTs (produced by the arc-discharge method) has been reported as 0.0074 L/(mg cm).[13] A higher estimated a_{SWNT} at 500 nm of 0.097 L/(mg cm) was reported for defunctionalized arc discharge prepared SWNTs.[18] The higher value was suggested to be due to scattering effects due to larger bundles. As has been suggested and observed in this study, values for a_{SWNT} at 500 nm can be

different for SWNTs prepared by the various methods, dispersal in the medium, light scattering contributions, etc..[13]

Eq 4 suggests that for an infinitely thin film (thickness approaching 0), as one that may be desired for certain types of Gossamer spacecraft, the absorbance would approach zero. Using this result in eq 2, the %T at 500 nm would be approximately 89%; independent of c_{SWNT}.

Of course, eq 4 for absorbance and %T (eq 2) are representative only of this particular batch of polymer-SWNT samples. The optical properties of samples prepared separately, or with different levels of quality control than those in this study, could deviate significantly from those reported herein. Additionally the data was obtained only as transmission measurements. Further experiments would need to be performed to determine if these results maybe due to scattering. Thus, caution should be exercised when applying this eq beyond the present data set. However, the overall methodology is sound and does provide a first-order predictive approximation that may be useful when applied to other systems.

Solar Absorptivity. As was found with absorbance, α (an absorptive property) was found to obey both Beer's and Lambert's laws. As previously mentioned, α encompasses the spectral region ranging from 250 to 2800 nm. A semi-empirical eq for α was chosen and best fit to the data using the Solver function in Microsoft Excel resulting in eq 5:

$$\alpha = 0.07230 + b[(0.000058\ \text{L/(mol}\ \mu\text{m))}c_{host} + (0.0740\ \text{L/(mol}\ \mu\text{m))}c_{SWNT}], \quad (5)$$

where c_{host} = 2.10 mol/L and b is in microns and c_{SWNT} is in mol/L. This formula predicts α with an uncertainty of ±0.01 with 95% confidence. Figure 4 shows good agreement between the data and eq 5 for films where the thickness was varied. Like absorbance, the α vs. c_{SWNT} relationship (P1-P4) was shown as a bar graph due to one sample not being of the same thickness.

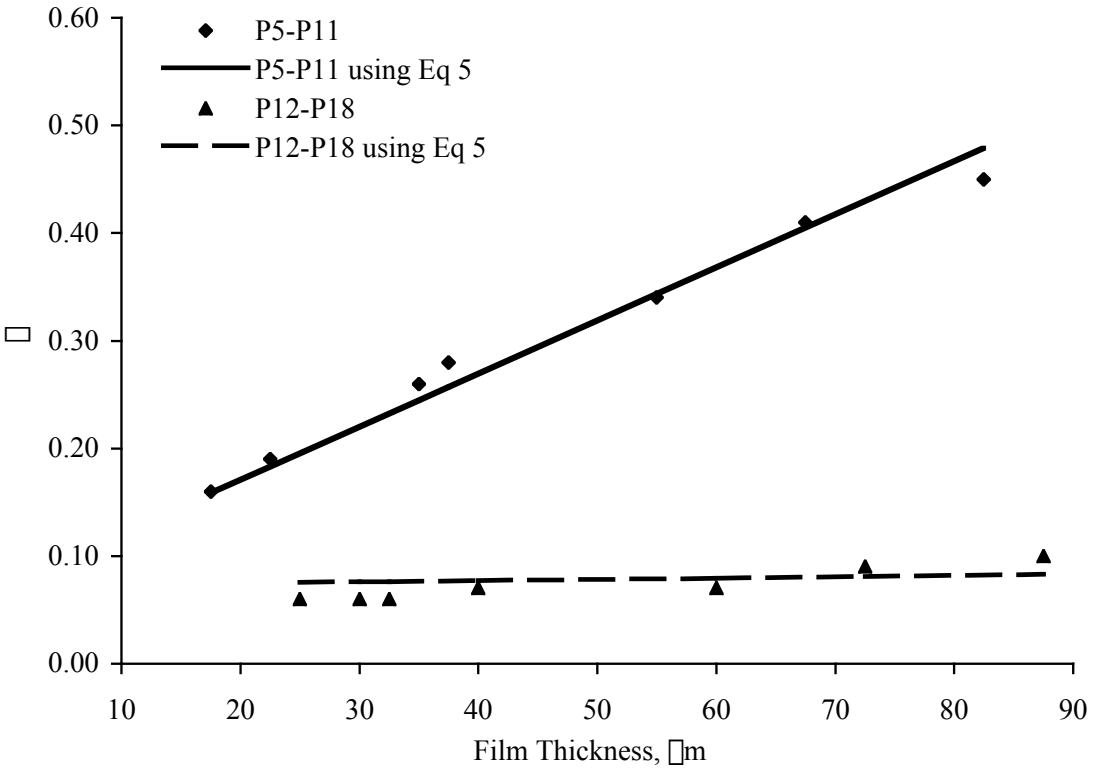

Figure 4. vs. film thickness for neat (P12-P18) and SWNT-loaded films (P5-P11).

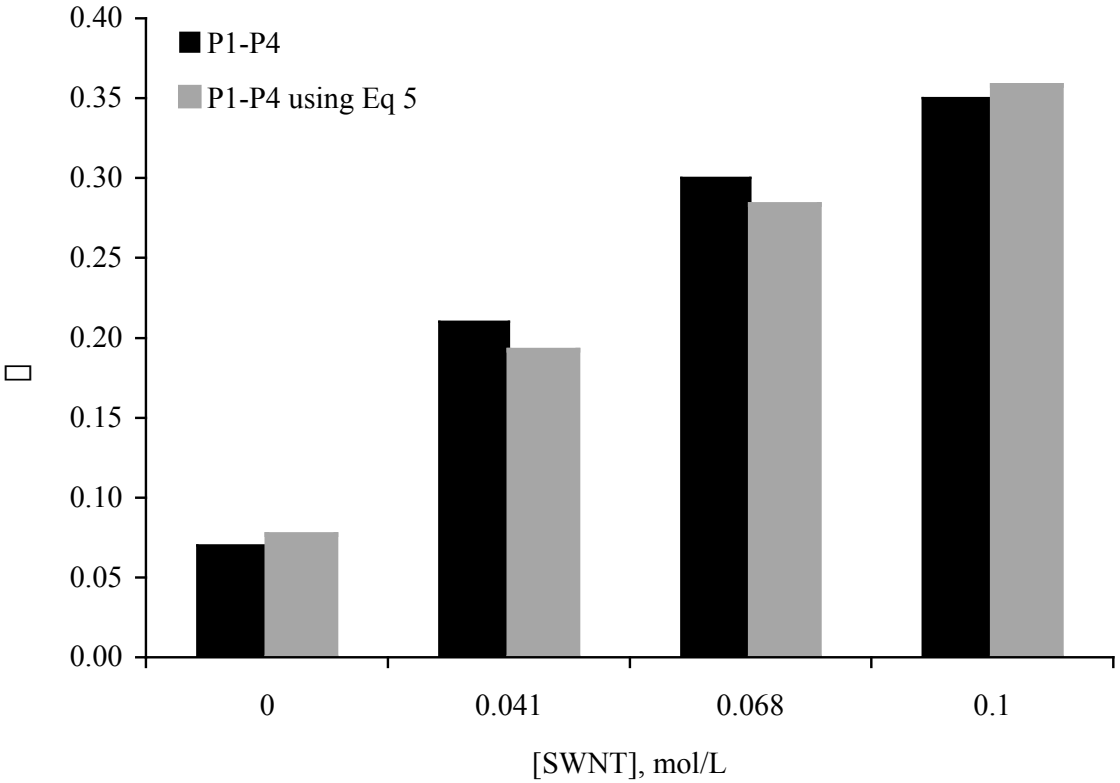

Figure 5. vs. c_{SWNT} for approximately constant thickness films (P1-P4).

Similar agreement was found by comparing eq 5 and data vs. c_{SWNT} (Figure 5).

Using eq 5, an infinitely thin film (thickness approaching 0) would exhibit an α of 0.07. This is independent of c_{SWNT} as seen for the absorbance (eq 4). Similar cautions and expectations as previously stated for the treatment of the absorbance data apply to the prediction of α by eq 5.

Emissivity. Even though ε is not an absorptive property, it was likewise examined to determine if a first order predictive eq could be developed. For each of the films, ε was measured and reported in Tables 1 and 2. An eq was developed with Microsoft Excel using the Solver function with the data fitted to a simple plane: an offset value of ε plus a linear term in each dimension of b and c_{SWNT}. The best fit function was (eq 6):

$$\varepsilon = 0.407 + 0.915c_{SWNT} + 0.0034b, \qquad (6)$$

where b was in microns and c_{SWNT} was in mol/L. Eq 6 was then plotted against the data in Figures 6 and 7. In general, eq 6 and the data agreed that ε increased with both film thickness and c_{SWNT}. However, there were some unexplained trends. It is unclear why there should be a nonlinearity in the ε as the film thickness decreased. Also, the data series shown in Figure 7 appeared to be systematically high (by about 0.05) compared to eq 6, which was fit to all of the data. There may have been a run-to-run variation either in the smaple preparation or in the measurement. Nonetheless, the trends identified appear sound. It is known though that the ε is dependent on many factors such as surface finish, color, oxidation, aging, etc. and hence maybe difficult to accurately model.

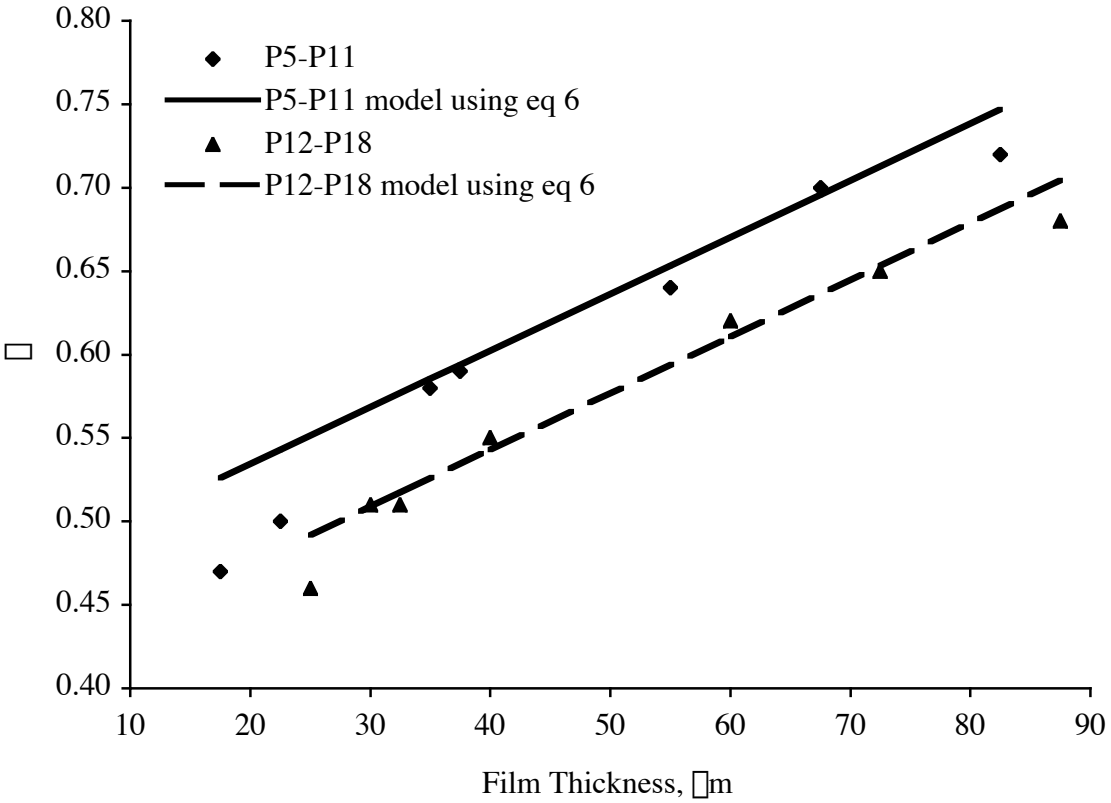

Figure 6. vs. film thickness for neat (P12-P18) and SWNT-loaded films (P5-P11).

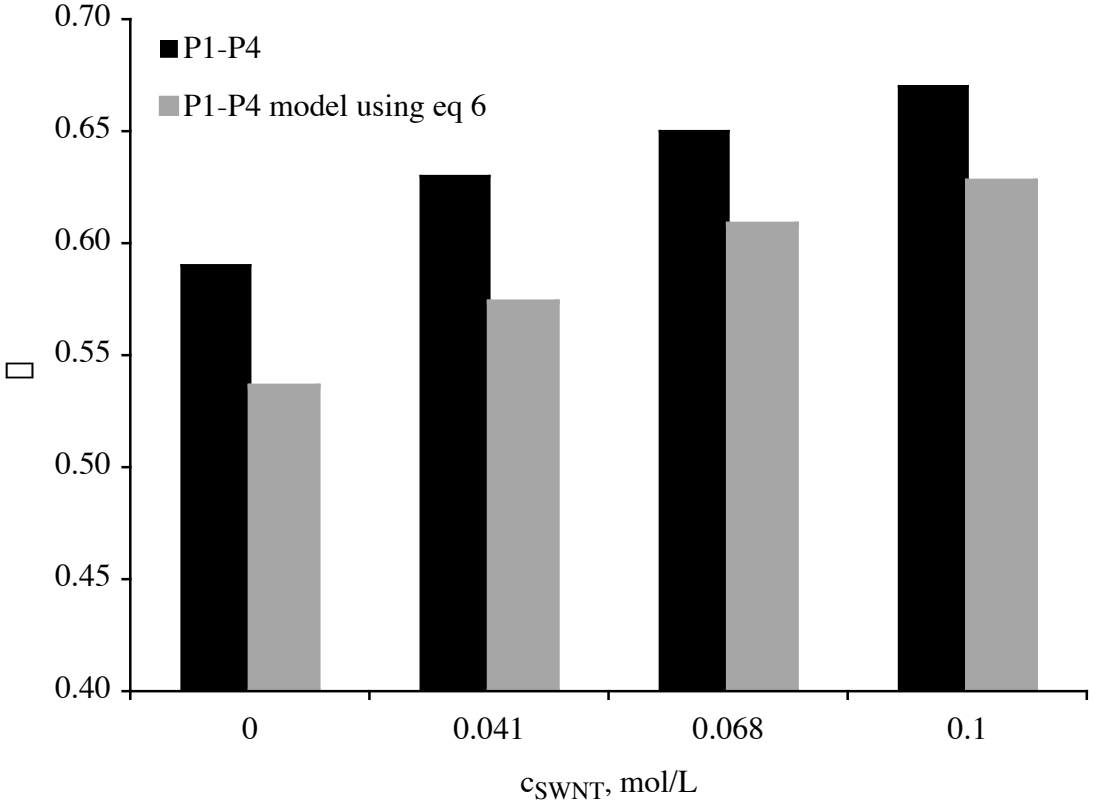

Figure 7. vs. c_{SWNT} for approximately constant thickness films (P1-P4).

SUMMARY

Optical and thermo-optical properties were measured for nanocomposite films prepared from alkoxysilane terminated amide acid polymers of LaRC™ CP-2 and HiPco SWNTs. Both film thickness and c_{SWNT} were varied. The absorbance at 500 nm and □ exhibited a linear dependence upon c_{SWNT} at constant film thickness and with varying film thickness at constant c_{SWNT}, respectively. These properties were found to obey Beer's and Lambert's laws, respectively. Empirical eqs were developed for absorbance at 500 nm and □ using the Solver function in Microsoft Excel. Predicted values for both were in good agreement with the data. The molar absorptivity at 500 nm determined for the HiPco SWNTs based on this approach was of the same order of magnitude as that determined for HiPco SWNTs in solution. An empricial eq was also developed for □, though it did not fit the data as satisfactorily as observed for the absorbance at 500 nm and □. This approach provides a first-order means to approximately predict both absorbance at 500 nm and □ (and possibly □) at various film thickness and SWNT loadings.

REFERENCES

1. Jenkins, CHM. *Gossamer Spacecraft: Membrane and Inflatable Structures Technology for Space Applications Vol. 191*; American Institute of Aeronautics and Astronautics, **2001**.
2. For an explaination of □ /square see Paasi, J. Research Note, http://www.vtt.fi/tuo/45/tuloksia/surface_resistance.pdf, March 19, 2002.
3. Watson, K.A.; Connell, J.W. *Polym. Mater. Sci. Eng. Proc.* **2001**, 46, 1853.
4. SRS Technologies, Huntsville, AL 35806, http://www.stg.srs.com/atd/polyimidesales/cp_prop.htm
5. Park, C.; Ounaies, Z.; Watson, K.A.; Crooks, R.E,.; Smith Jr., J.G.; Lowther, S.E.; Connell, J.W.; Siochi, E.J.; Harrison, J.S.; St. Clair, T.L. *Chem. Phys. Lett.* **2002**, 364, 303.

6. Watson, K.A,.; Smith Jr., J.G.; Connell, J.W. *Society for the Advancement of Materials and Process Engineering Technical Conference Series* **2001**, 33, 1551.
7. Smith Jr., J.G.; Watson, K.A,.; Thompson, C.M.; Connell, J.W. *Society for the Advancement of Materials and Process Engineering Technical Conference Series* **2002**, 34, 365.
8. Glatkowski, P.; Mack, P.; Conroy, J.L.; Piche, J.W.; Winsor, P. *U.S. Patent 6,265,466 B1*; **July 24, 2001**.
9. Ounaies, Z.; Park, C,.; Wise, K.E.; Siochi, E.J.; Harrison, JS. *Comp. Sci. and Tech.* **2003**, 63, 1637.
10. Smith Jr., J.G.; Connell, J.W.; Delozier, D.M.; Lillehei, P.T.; Watson, K.A.; Lin, Y.; Zhou, B,.; Sun, Y-P. *Polymer*. **2004**, 45, 825.
11. Watson, K.A.; Smith Jr., J.G.; Connell, J.W. *Society for the Advancement of Material and Process Engineering Proceedings* **2003**, 48, 1145.
12. Bahr, J.L.; Mickelson, E.T.; Bronikowski, M.J,.; Smalley, R.E.; Tour, J.M. *Chem. Commun.* **2001**, 193.
13. Bing, Z.; Lin, Y.; Huaping, L.; Huang, W.; connell, J.W.; Allard, L.F.; Sun, Y-P. *J. Phys. Chem. B* **2003**, 107, 13588.
14. Hu, H.; Bhowmik, P.; Zhao, B.; Hamon, M.A.; Itkis, M.E.; Haddon, R.C. *Chem. Phys. Lett.* **2001**, 345,25.
15. Mawhinney, D.B.; Naumenko, V.; Kuznetsova, A.; Yates, J.T.; Liu, J.; Smalley, R.E. *Chem. Phys. Lett.* **2000**, 324,213.
16. Hull CC and Crofts NC. *Ophthal. Physiol. Opt.* **1996**, 16,150.
17. a) Meyer-Arendt, JR. *Introduction to Classical and Modern Optics*, Prentice-Hall Inc. **1972**, pp. 305-311. b) Hecht, E. *Optics 4th Ed.*, Pearson Addison Wesley **2001.**
18. Fu, K.; Huang, W.; Lin, Y.; Riddle, L.A.; Carroll, D.L.,; Sun, Y-P. *Nano Lett.* **2001**, 1, 439.